TECHNIUM

Romanian Journal of Applied Sciences and Technology
ISSN: 2668-778X

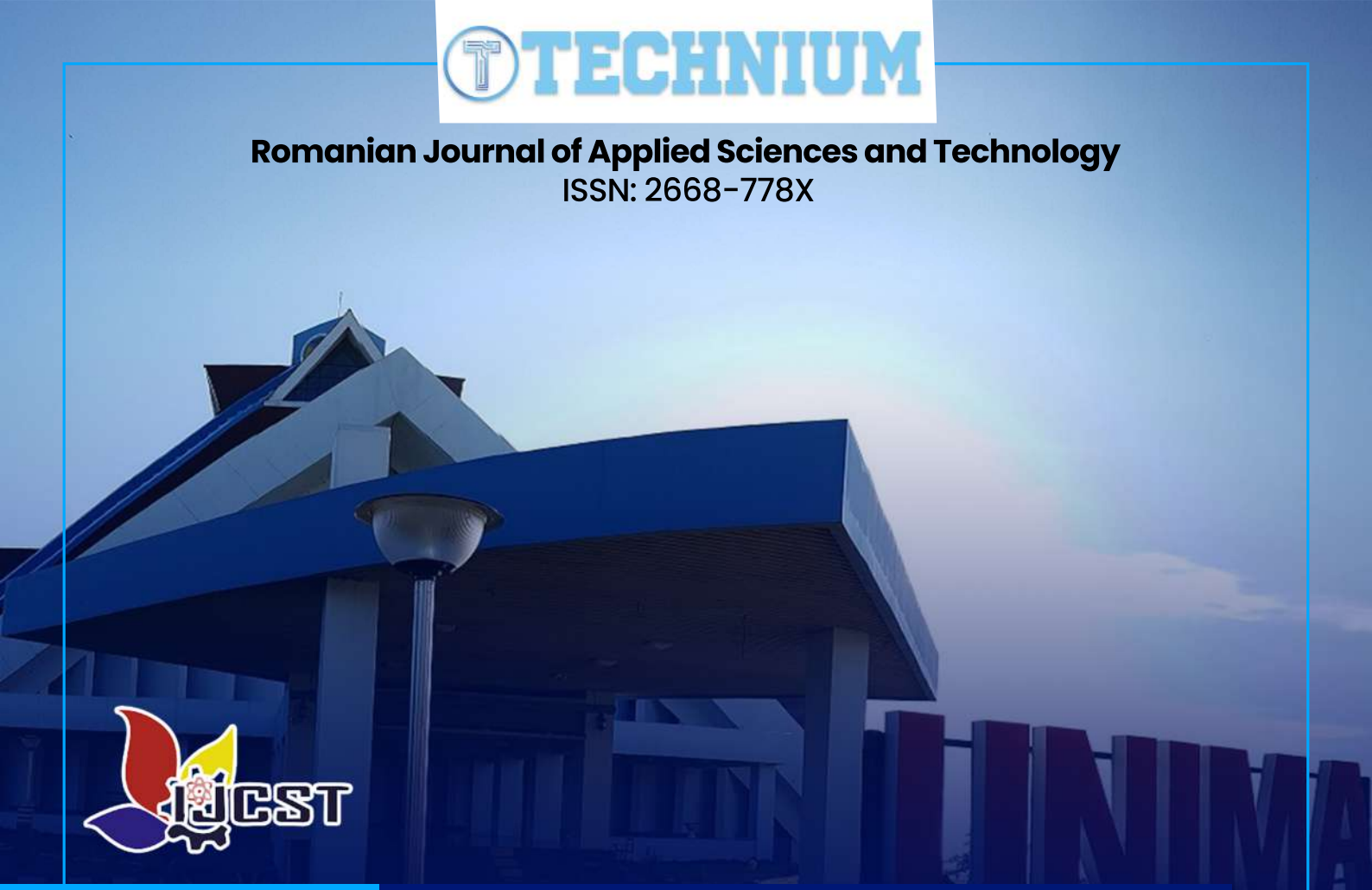

vol. 16 / 2023

The 7th International Conference on Science Technology

organized by
Faculty of Social Science and
Law Universitas Negeri Manado and
Consortium of International Conference
on Science and Technology

The Innovation Breakthrough in Digital and Disruptive Era

Technium: Romanian Journal of Applied Sciences and Technology
Vol. 16, 310-316, October, 2023
ISSN: 2668-778X
www.techniumscience.com

Multiphase Flow Analysis of Three-Dimensional Journal Bearing with Roughness Using Computational Fluid Dynamics (CFD)

S Susilowati[1,2 *], *Silvana Dwi Nurherdiana*[1,2], *,Sukirmiyadi*[1], *Erwan Adi Saputro*[1,2] *Mohammad Tauviqirrahman*[3], *Dani Arfiandani*[3] , and *Paryanto*[3,4]

[1]Master of Environmental Science, Faculty of Engineering, Universitas Pembangunan Nasional Veteran Jawa Timur, Surabaya, Indonesia
[2]Study Program of Chemical Engineering, Faculty of Engineering, Universitas Pembangunan Nasional Veteran Jawa Timur, Surabaya, Indonesia
[3]Department of Mechanical Engineering, Diponegoro University, Jl. Soedharto SH, Tembalang, Semarang 50275, Indonesia
[4]Institute for Factory Automation and Production Systems (FAPS), Friedrich-Alexander-Universität Erlagen-Nürnberg, Egerlandstr. 7-9, Erlangen, 91058, Germany

Abstract. Investigating the impact of surface roughness characteristics on three-dimensional journal bearings while adjusting the eccentricity ratio is the primary goal of this work. Based on computational fluid dynamics, the rotor-bearing system with sand-grain roughness distribution surface is investigated (CFD). To study the tribological performance, the Reynolds-Average Navier-Stokes equations are combined with a multi-phase cavitation model (hydrodynamic pressure, load support and friction). The calculation demonstrates that the surface roughness level in relation to friction and load support is a determining factor for journal bearing performance

* Corresponding author: susilowati.tk@upnjatim.ac.id

Technium: Romanian Journal of Applied Sciences and Technology
Vol. 16, 310-316, October, 2023
ISSN: 2668-778X
www.techniumscience.com

1 Introduction

The examination of bearing performance in classical hydrodynamic lubrication theory frequently makes the assumption that the surface is totally smooth. This assumption is unfounded since all surfaces at the microscale are inherently rough. As a result, numerous research on the impact of surface roughness have been published. It has been established, as is common knowledge, that surface roughness affects how much lubricant forms on a given surface as well as how well a bearing performs under hydrodynamic pressure.

Using Christensen's stochastic theory, Gururajan and Prakash [1-3]. studied the impact of surface roughness in a narrow porous journal bearing under hydrodynamic conditions. Naduvinaman and his team investigated the combined impact of the couple stresses and surface roughness of the bearing on the lubrication performance for the cases of journal bearings [4] and slider bearings [4-5] using the same rough surface theory in the presence of couple stress fluid. Bujurke et al. [6] investigated the effects of surface roughness on the properties of squeeze film lubrication between curved annular plates for pure squeeze film problems. The load support due to the combined impacts of roughness and heat is less for nonparallel slider bearing, according to an intriguing study by Deresse and Sinha [7], for both longitudinal and transverse roughness models. They used the stochastic Gaussian random distribution to model the roughness in their work. Regarding the temperature effect, Zhao et al. [8] discovered a different outcome. They got to the conclusion that the impact of surface roughness on bearing performance diminished when heat and elastic deformation were taken into account simultaneously. According to Kalavathi [9] for the bearing with heterogeneous slip/no-slip surface, pressure profile and load support rise with increasing roughness. Based on the mixed elasto-hydrodynamic lubrication model, Zhang et al. [10] investigated the impact of the rough surface on tribological behaviors. The authors came to the conclusion that increased roughness increases friction coefficient. By taking into account the bearing deformation [11], the shape of the roughness [12], and the thermal effect [13], Kumar and his team, evaluated the impact of the surface roughness. Their key discovery was that the temperature and roughness have a significant impact in pressure creation.

Numerous studies have been conducted to portray the surface roughness in order to comprehend some journal bearing qualities. For instance, Sugimura et al. [14] conducted an experimental study to determine the impact of surface roughness pattern on the lubricated running-in procedure in the case of pure rolling/sliding contact. The authors came to the conclusion that very thin stable films are produced via longitudinal roughness. Cui et al. [15] later came to the conclusion that the surface roughness has a substantial impact on the transient characteristics of the bearing during the initial phase of startup using the Greenwood-Williamson (GW) contact model. The effect of surface roughness on the start-stop behavior of air-lubricated thrust micro-bearings was examined by Zhang et al. [15]. Their findings demonstrated that a rise in the asperity height's standard deviation causes a fall in the air bearing force. In a recent article, Yin et al. [16] noted that the connection between the roughness distribution and surface textures was complex for the situation of textured bearing. They demonstrated that combining surface texturing with roughness (in their case, a modest negative skewness surface) could improve lubrication performance using real non-Gaussian roughness distribution liners.

The relationship between surface roughness and eccentricity ratio for the lubricated journal bearing has not yet been fully studied. In the current study, an effort has been made to investigate how surface roughness affects the lubrication characteristics of three-dimensional length journal bearings by taking multi-phase cavitation into account. It is also described how the eccentricity ratio affects the hydrodynamic pressure, load support, and friction aspects of lubrication performance. Additionally, this research differs from others in that the sand-grain model is being used to model roughness.

2 Method

2.1 Governing Equations

Using the Reynolds equation and the results of the literature review, it was discovered that the surface roughness has a significant impact on lubrication . However, computational fluid dynamics analysis (CFD) is used to explore in greater depth the impact of surface roughness in the presence of inertia. The CFD software program FLUENT® is a commercial product. After being solved, the Navier-Stokes and continuity equations can each be stated as follows:

$$\rho \frac{Du_i}{Dt} = -\frac{\partial p}{\partial x_i} + \rho G_i + \frac{\partial}{\partial x_j}\left[2\eta e_{ij} - \frac{2}{3}\eta(\nabla . u_i)\delta ij\right] \quad (1)$$

$$\nabla \bullet \mathrm{u} = 0 \quad (2)$$

The multi-phase cavitation model is utilized to get more representative results because cavitation occurs throughout the diverging zone of the bearing. The multi-phase cavitation model, in contrast to Reynolds cavitation model, permits lubricant phase shift. The Zwart-Gelber-Belamri method is used in the current work to model cavitation in order to produce accurate results quickly. The vapor transport equation governs the liquid-vapor mass transfer (evaporation and condensation) in cavitation:

$$\frac{\partial}{\partial t}(\alpha_v \rho_v) + \nabla . (\alpha_v \rho_v v) = R_g - R_c \quad (3)$$

where α_v refers to vapour volume fraction and ρ_v account for vapor density. R_g and R_c denote for the mass transfer between the liquid and vapour phases in cavitation. For Zwart-Gelber-Belamri model, the final form of the cavitation is as follows:

$$p \le p_v, R_g = F_{evap}\frac{3\alpha_{\mathrm{nuc}}(1-\alpha_v)\rho_v}{R_B}\sqrt{\frac{2}{3}\frac{P_v - P}{\rho_\ell}} \quad (4)$$

TECHNIUM
Technium: Romanian Journal of Applied Sciences and Technology
Vol. 16, 310-316, October, 2023
ISSN: 2668-778X
www.techniumscience.com

$$p \geq p_v, R_c = F_{cond} \frac{3\alpha_v \rho_v}{R_B} \sqrt{\frac{2}{3} \frac{P - P_v}{\rho_\ell}} \quad (5)$$

where F_{evap} = evaporation coefficient = 50, F_{cond} = condensation coefficient = 0.01, R_B = bubble radius = 10-6 m, α_{nuc}= nucleation site volume fraction= $5x10^{-4}$, ρ_l = liquid density and P_v = vapor pressure. It is noteworthy that the computational results of the present work are limited to the hydrodynamic regime of lubrication.

2.2 Roughness Modeling

The sand-grain model is used in this study to describe the bearing surface's roughness distribution. The modified law-of-the-wall for mean velocity is utilized to model the roughness, according to ANSYS FLUENT®. It states:

$$\frac{u_p u^*}{\tau_w/\rho} = \frac{1}{\kappa} ln\left(E \frac{\rho u^* y_p}{\eta}\right) - \Delta B \quad (6)$$

where $u^* = C_\eta^{1/4} \kappa^{1/2}$ and $\Delta B = (1/\kappa) \ln f_r$. f_r refers to the roughness function. For sand-grain roughness, ΔB is affected by the physical roughness height K_s. Based on the work of Adams et al., the roughness height K_s can be correlated with the value of the average roughness R_a measured by profilometer as follows:

$$K_s = 0.5863 R_a \quad (7)$$

This equation allows the effect of the geometrical average roughness Ra of the surface can be calculated. In this study, for simplicity the uniform sand-grain roughness is assumed.

2.3 CFD Model

Fig. 1. depicts a journal bearing's schematic diagram. While the entire bearing surface is deemed to be rough, the shaft surface is thought to be absolutely smooth (θ = 0-360°). As mentioned in the previous section, the roughness level is expressed with Ra (i.e. average roughness). There are two levels of roughness considered here, i.e. Ra = 0.1 µm (precise) and Ra = 12.5 µm (rough). Additionally, in this work the eccentricity ratio is varied to obtain the understanding the effect of surface roughness in different loadings.

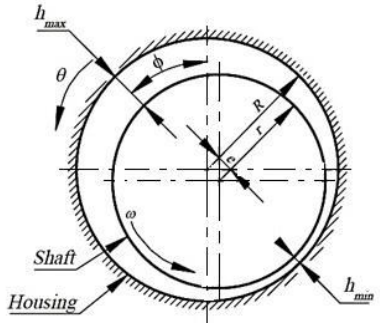

Fig. 1. Division of the bearing geometry into three parts

The parameters used in the simulations is shown in Table 1. The continuity equation and the Navier-Stokes equations are solved in this study utilizing the finite volume approach and the second-order spatial accuracy of the SIMPLE algorithm. To discretize the computational domain, which measures 800 x 80 x 36 along the circumferential, width, and radial directions of the journal bearing, the lubricant film is meshed using the hexahedral element produced by ANSYS's ICEM CFD module.

Table 1. Model Parameters

Parameter	Symbol	Value
Housing radius	R	50.145 mm
Shaft radius	r	50 mm
Bearing length	L	100 mm
Bearing clearance	c	0.145 mm
Eccentricity ratio	ε	0.41; 0.61; and 0.81
Density of lubricant vapor	ρ_{sat}	2 x 10^5 Pa-s
Viscosity of lubricant vapor	η_{sat}	1.2 kg/m^3
Saturation pressure of vapor	P_{sat}	20.000 Pa
Lubricant density	ρ	840 kg/m^3
Lubricant viscosity	η	0.0127 Pa-s

3 Results and Discussion

3.1. Surface Roughness and Eccentricity

Due to varying levels of surface roughness, the surface finishing process used in the production of bearings may produce surprising surface patterns. In this section, the impact of surface roughness on lubrication performance will be assessed. Fig. 2. displays the hydrodynamic pressure profile along the circumferential direction for two different roughness levels at various eccentricity ratios. Three specific features can be made based on Fig. 2. First, in the case of "precise" journal bearing (R_a = 0.1 µm in this case), the increase in the eccentricity ratio generates the increase in the hydrodynamic pressure profile as well as the pressure peak. This is to be expected because a lower eccentricity ratio results in less bearing loading.

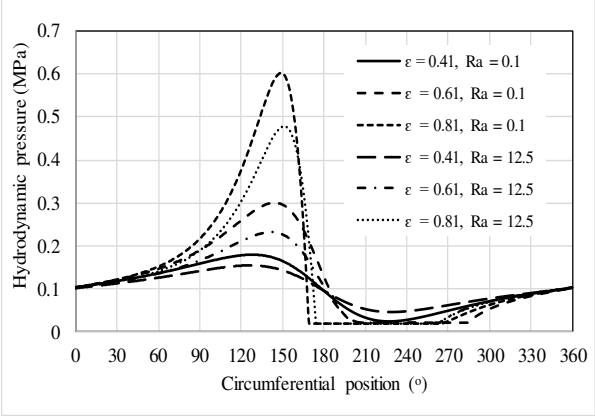

Fig. 2. Hydrodynamic pressure distribution varying eccentricity ratios ε and roughness levels Ra. All results are evaluated at z / L = 0.5.

As a result, the wedge effect will be less and lubrication pressure will be reduced. Second, in the case of "rough" journal bearing (R_a = 12.5 µm in this case), the effect of surface roughness has a same trend with the case of "precise" journal bearing, i.e. higher-pressure profile for larger eccentricity ratio. Third, it can be seen that, for a certain eccentricity ratio (i.e.,

Technium: Romanian Journal of
Applied Sciences and Technology
Vol. 16, 310-316, October, 2023
ISSN: 2668-778X
www.techniumscience.com

bearing loading), the peak pressure drops when the level of surface roughness is raised. It means that the bearing's surface roughness causes a decrease in pressure, which results in a reduced load support. The bearing surface should be properly constructed from a manufacturing standpoint to attain the desired surface roughness. Because an improper finishing technique for the bearing surface causes the lubrication performance to decline, the bearing's lifespan eventually gets shorter.

Fig. 3. detailed representation of the hydrodynamic pressure on the bearing's inner surface at various eccentricity ratios and roughness levels. The pressure peak appears in several places, as shown in Fig. 3., depending on the eccentricity ratio's magnitude. For example, for case of "$\varepsilon = 0.81$", the pressure peak is located at θ of $150°$, while for low eccentricity ratio, say $\varepsilon = 0.41$, the pressure peak occurs at θ of $130°$. Additionally, it can be seen that for any eccentricity ratio, the position of the peak pressure is constant regardless of the roughness level. On the basis of Fig. 3., it is also discovered that the zone of high pressure increases with decreasing eccentricity ratio. This pattern is consistent for the two roughness levels examined here. For example, in the case of "rough" surface, for low eccentricity ratio ($\varepsilon = 0.41$ in this case), the high-pressure zone exists at the position θ of $90°$-$160°$, while for case of high eccentricity ratio (i.e. $\varepsilon = 0.81$), the high-pressure zone reduces by up to 60% (i.e. position of 120°-170°). However, the bearing with the high eccentricity ratio is able to provide the highest value in terms of the expected highest pressure (200% and 50% greater in comparison to the cases of low and medium eccentricity ratio, respectively).

The hydrodynamic pressure is shown to be affected by surface roughness in terms of its value but not its position in Fig. 3 to 8. For the case of medium low eccentricity ratio studied here ($\varepsilon = 0.61$ in this case), the high-pressure zone is found in the same position (i.e. 100°-160°) both for smooth surface (R_a = 0.1 µm) and rough surface (R_a = 12.5 µm). The maximum hydrodynamic pressure appears to be 22% higher for "precise" surfaces compared to "rough" surfaces, nevertheless. The most likely explanation is that the hydrodynamic pressure falls because the flow gap causes a sequence of constrictions in the film as the roughness increases and the fluid moves in a circular direction.

3.2. On the Cavitation Phenomena

Fig. 9 to 14 depicts the volume fraction of lubricant vapor at various roughness values while adjusting the eccentricity ratios in order to explain the impact of surface roughness on the cavitation processes. The rationale for this is because the presence of vapor in a specific location indicates the cavitation process is real. It is obvious that the volume proportion of vapor is produced much more when the eccentricity ratio is high. From a physical standpoint and in an equilibrium condition, the so-called "cavitation" phenomena causes a rise in the value of the pressure at the other place to make up for the decrease in pressure caused by the cavitation's existence. Because of this, a bearing with a high eccentricity ratio generates more pressure, which improves load support. Figures 9 to 14 show that the surface roughness effect causes smoother surfaces to produce more vapor than rough surfaces do. On the other hand, as the level of roughness increases, less cavitation occurs, resulting in less load support.

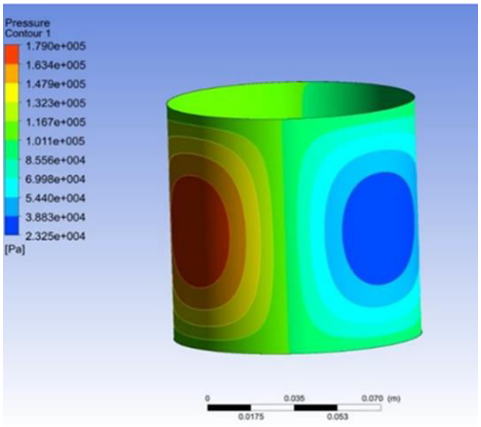

Fig. 3. Contour of hydrodynamic pressure for several cases: $\varepsilon = 0.41$ and $R_a = 0.1$ µm

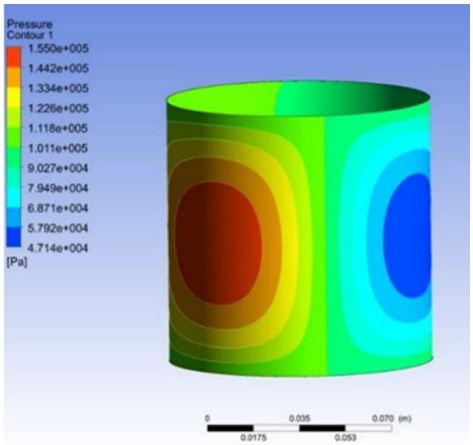

Fig. 4. Contour of hydrodynamic pressure for several cases: $\varepsilon = 0.41$ and $R_a = 12.5$ µm

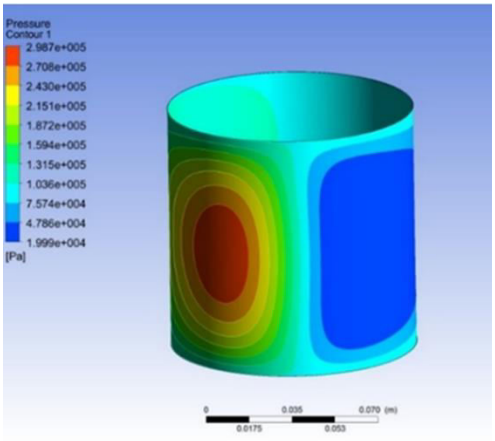

Fig. 5. Contour of hydrodynamic pressure for several cases: $\varepsilon = 0.61$ and $R_a = 0.1$ µm

Technium: Romanian Journal of
Applied Sciences and Technology
Vol. 16, 310-316, October, 2023
ISSN: 2668-778X
www.techniumscience.com

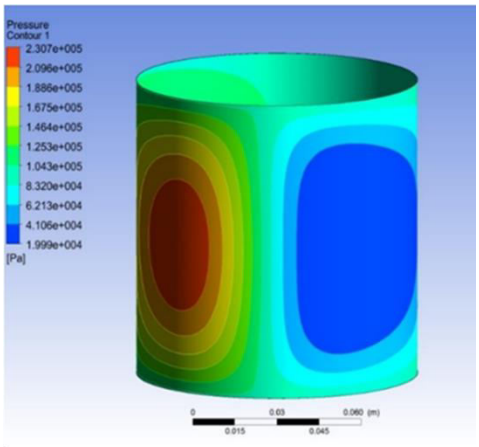

Fig. 6. Contour of hydrodynamic pressure for several cases: $\varepsilon = 0.61$ and $R_a = 12.5$ µm

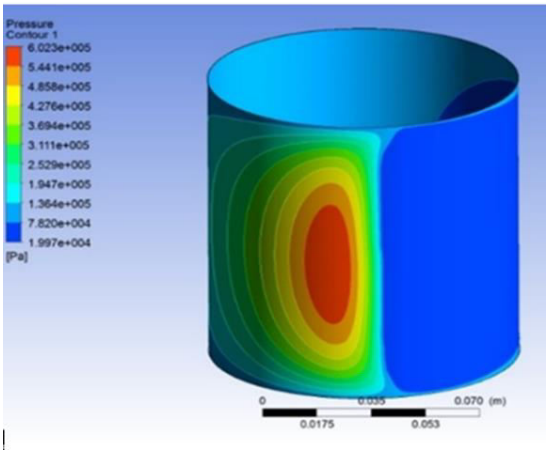

Fig.7. Contour of hydrodynamic pressure for several cases: $\varepsilon = 0.81$ and $R_a = 0.1$ µm

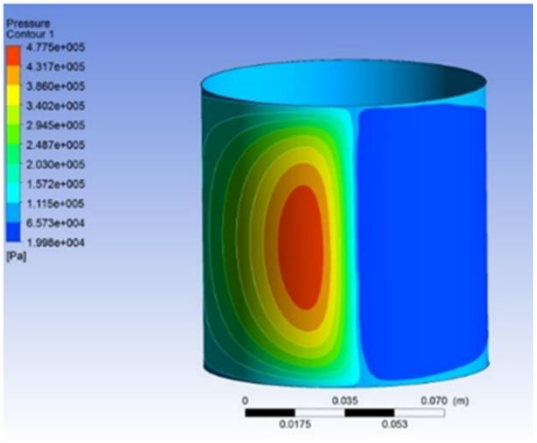

Fig. 8. Contour of hydrodynamic pressure for several cases: $\varepsilon = 0.81$ and $R_a = 12.5$ µm

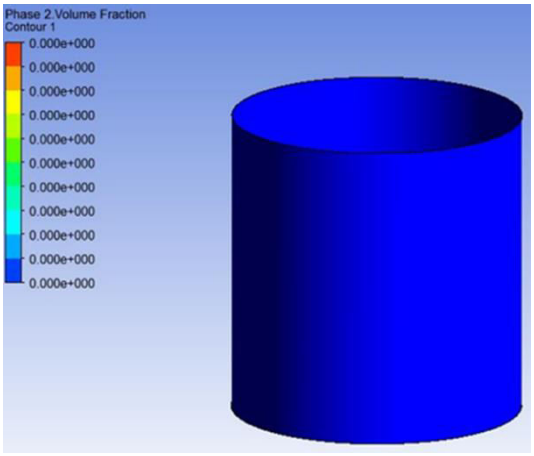

Fig. 9. Contour of volume fraction of vapor for several cases: $\varepsilon = 0.41$ and $R_a = 0.1$ µm

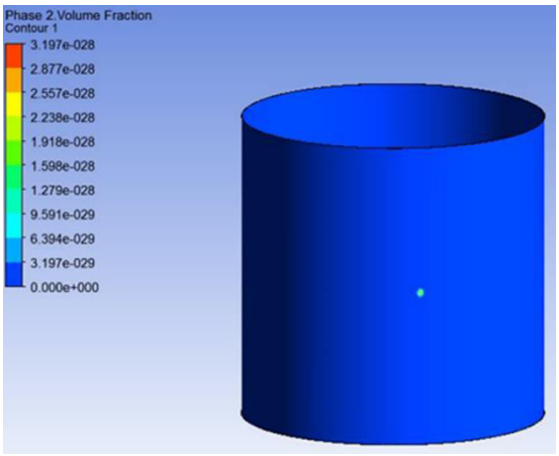

Fig. 10. Contour of volume fraction of vapor for several cases: $\varepsilon = 0.41$ and $R_a = 12.5$ µm

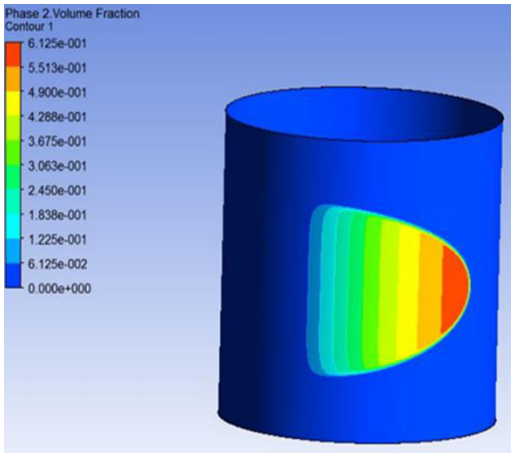

Fig. 11. Contour of volume fraction of vapor for several cases: $\varepsilon = 0.61$ and $R_a = 0.1$ µm

Technium: Romanian Journal of Applied Sciences and Technology
Vol. 16, 310-316, October, 2023
ISSN: 2668-778X
www.techniumscience.com

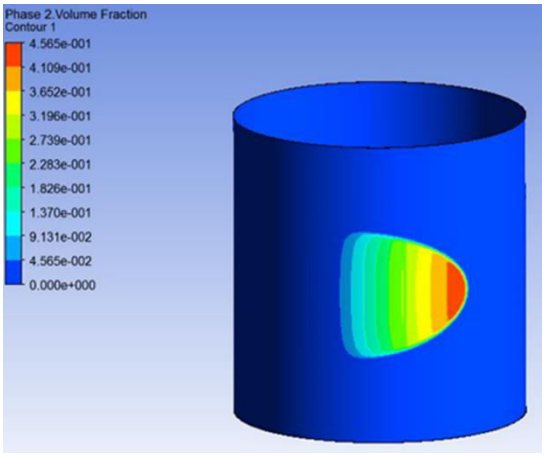

Fig. 12. Contour of volume fraction of vapor for several cases: $\varepsilon = 0.61$ and $R_a = 12.5$ µm

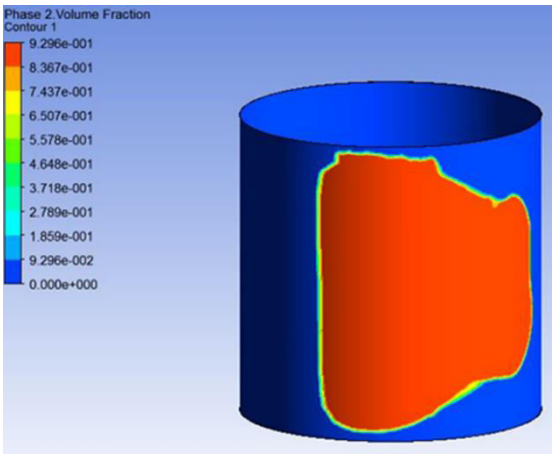

Fig. 13. Contour of volume fraction of vapor for several cases: $\varepsilon = 0.81$ and $R_a = 0.1$ µm

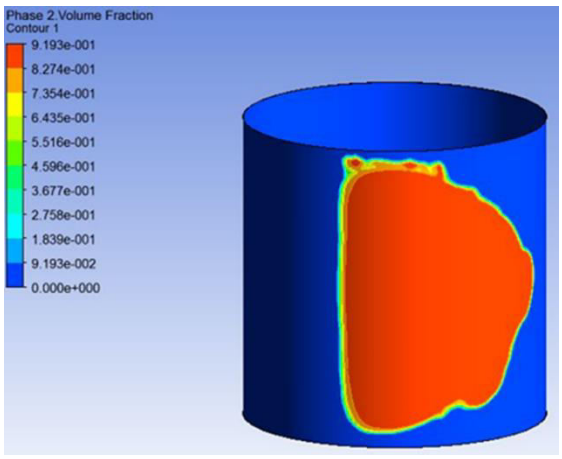

Fig. 14. Contour of volume fraction of vapor for several cases: $\varepsilon = 0.81$ and $R_a = 12.5$ µm

3.3. On the Load Support and Friction Force

Calculating the friction and load support will reveal the three- dimensional journal bearing's lubrication performance. While the friction force is derived by integrating the shear stress along the surface area, the load support is defined as an integration of hydrodynamic pressure along the surface area. Fig. 15 depicts the effect of eccentricity ratio on the load support for two different roughness levels ($R_a = 0.1$ µm and 12.5 µm). In terms of the load support, it can be shown that for small eccentricity ratio ($\varepsilon = 0.41$ in this case), the roughness level effect is not significant so much. On the other words, the "smooth" surface (i.e. $R_a = 0.1$ µm) and the "rough" surface ($R_a = 12.5$ µm) generates the same value of the predicted load support of the bearing. From the physical point of view, this is because the volume fraction of vapor generated for both cases (i.e. $R_a = 0.1$ and 12.5 µm for $\varepsilon = 0.41$) is relatively very small as depicted in Fig. 9 to Fig 10. With respect to the effect of eccentricity ratio, from Fig. 15 it can be also found that increasing the eccentricity ratio increases the load support.

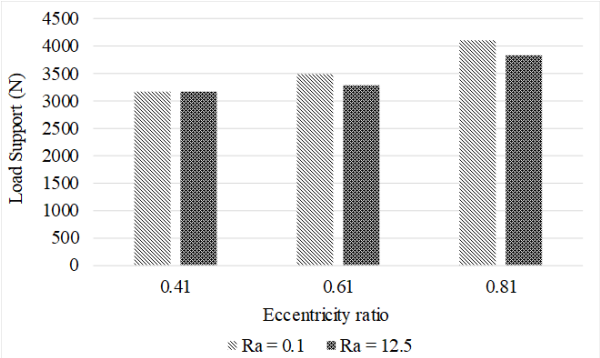

Fig. 15. Effect of eccentricity ratio on the load support for two different roughness levels.

For example, for the case of $R_a = 0.1$ µm, the load support predicted by "ε = 0.41" case differs by 22 % (lower) compared to prediction of ε = 0.81 case. Fig. 15 also reflects that in the case of high eccentricity ratio, i.e. ε = 0.61 and 0.81, the roughness level effect on the load support is highlighted. Based on Fig. 15, it is observed that when the surface roughness falls into the "rough" level (i.e. $R_a = 12.5$ µm), the load support decreases by 7% both for the case of eccentricity ratio of 0.61 and 0.81. In general, it is advised to carefully produce the bearing surface roughness level for bearings designed to function under high loads (i.e., high eccentricity ratio) in order to ensure the best lubrication performance.

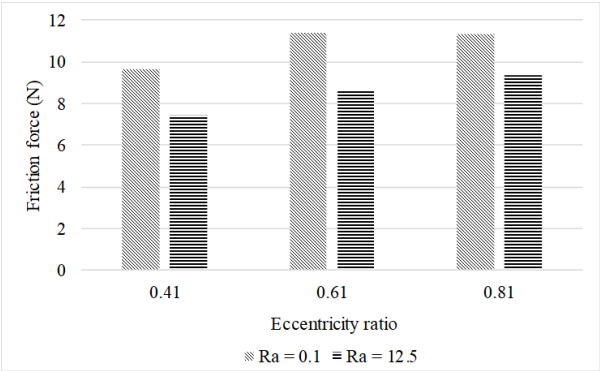

Fig. 16. Effect of eccentricity ratio on the friction for two different roughness levels

Fig. 16 illustrates how surface roughness affects eccentricity ratio values in response to friction force. According to Fig. 16, the performance of friction varies significantly for the same eccentricity ratio. Depending on the value of the eccentricity ratio, it ranges from 21 to 32%. It is obvious that if the greased surface of the bearing is configured to be rougher, the friction force is lowered. These findings are intriguing because in practical applications, a bearing's ability to simultaneously generate strong load support and minimal friction force must be good. In order to achieve high load support but low friction force, future work should take into account the optimization of the roughness level as an interesting challenge.

4 Conclusion

In this study, the impact of bearing surface roughness on tribological performance was examined utilizing the CFD approach and industry-standard software ANSYS FLUENT®. The multi-phase cavitation model was coupled with research on lubricant phase change. The simulation findings demonstrate that raising the eccentricity ratio increases load support when the bearing is rough. Another intriguing discovery is that roughness has two opposing impacts, lowering load support (i.e., a negative effect) and increasing friction force (i.e., a positive effect), simultaneously. In order to achieve the best roughness and eccentricity ratio, which results in good load support yet minimal friction, optimization research should be done.

5 References

[1] Gururajan, K., Prakash, J., 1999. Surface roughness effects in infinitely long porous journal bearings. J. Tribol. 121, 139–147.

[2] Gururajan, K., Prakash, J., 2000. Effect of surface roughness in a narrow porous journal bearing. J. Tribol. 122, 472–475.

[3] Gururajan, K., Prakash, J., 2002. Roughness effects in a narrow porous journal bearing with arbitrary porous wall thickness. Int. J. Mech. Sci. 44, 1003–1016.

[4] Naduvinamani, N.B., Fathima, S.T., Hiremath, P.S., 2003. Hydrodynamic lubrication of rough slider bearings with couple stress fluids. Tribol. Int. 36, 949–959.

[5] Naduvinamani, N.B., Siddangouda, A., 2007. Effect of surface roughness on the hydrodynamic lubrication of porous step-slider bearings with couple stress fluids. Tribol. Int. 40, 780–793.

[6] Bujurke, N.M., Naduvinamani, N.B., Basti, D.P., 2007. Effect of surface roughness on the squeeze film lubrication between curved annular plates. Ind. Lubr. Tribol. 59, 178–185.

[7] Deresse, G.A., Sinha, P., 2011. THD analysis for finite slider bearing with roughness: Special reference to load generation in parallel sliders. Acta Mech. 222, 1–15.

[8] Zhao, X., Sun, J., Wang, C., Wang, H., Deng, M., 2013. Study on thermoelastohydrodynamic performance of bearing with surface roughness considering shaft deformation under load in shaft-bearing system. Ind. Lubr. Tribol. 65, 119–128.

[9] Kalavathi, G.K., Dinesh, P.A., Gururajan, K., 2016. Influence of roughness on porous finite journal bearing with heterogeneous slip/no-slip surface. Tribol. Int. 102, 174–181.

[10] Zhang, H., Dong, Guangneng, Dong, Guozhong, 2018. A mixed elastohydrodynamic lubrication model based on virtual rough surface for studying the tribological effect of asperities. Ind. Lubr. Tribol. 70, 408–417.

[11] Kumar, R., Azam, M.S., Ghosh, S.K., Khan, H., 2017. Effect of surface roughness and deformation on Rayleigh step bearing under thin film lubrication. Ind. Lubr. Tribol. 69, 1016–1032.

[12] Kumar, R., Azam, M.S., Ghosh, S.K., Khan, H., 2019. Performance evaluation of rough thrust pad bearing under thermo-elastohydrodynamic lubrication using an improved iterative method. Mech. Ind. 20.

[13] Kumar, R., Ghosh, S.K., Azam, M.S., Khan, H., 2020. Numerical Simulation of Rough Thrust Pad Bearing Under Thin-Film Lubrication Using Variable Mesh Density. Iran. J. Sci. Technol. - Trans. Mech. Eng. 44, 443–464.

[14] Sugimura, J., Watanabe, T., Yamamoto, Y., 1994. Effects of surface roughness pattern on the running-in process of rolling/sliding contacts. Tribol. Ser. 27, 125–137.

[15] Cui, S., Gu, L., Fillon, M., Wang, L., Zhang, C., 2018. The effects of surface roughness on the transient characteristics of hydrodynamic cylindrical bearings during startup. Tribol. Int. 128, 421–428.

[16] Yin, B., Zhou, H., Xu, B., Jia, H., 2019. The influence of roughness distribution characteristic on the lubrication performance of textured cylinder liners. Ind. Lubr. Tribol. 71, 486–493.